Multi-step Boris rotation schemes for Lorentz force equation of charged particles

Takayuki Umeda

Institute for Space-Earth Environmental Research, Nagoya University, Nagoya City, Aichi 464-8601, JAPAN

Abstract

A numerical procedure for integrating the rotation equations of electrically charged particles in magnetic fields with higher accuracy is provided. The proposed n-step rotation schemes have the same accuracy with the standard Boris rotation with $1/2^{n-1}$ time step.

Keywords: Boris integrator; Lorentz force equation; Higher accuracy

1. Introduction

The particle-in-cell method has now become an essential approach for studying space plasmas processes. The particle-in-cell method is established in early 1980's [1, 2]. The Boris integrator (or the Boris push) [3] is one of the most fundamental numerical scheme, which integrate the acceleration equations of electrically charged particles in electromagnetic fields.

The starting point is the Coulomb-Lorentz equation which expresses the acceleration of charged particles by the Coulomb-Lorentz force

$$\frac{\mathrm{d}}{\mathrm{d}t}(m\boldsymbol{v}) = q(\boldsymbol{E} + \boldsymbol{v} \times \boldsymbol{B}). \tag{1}$$

The central time difference of Eq.(1) is written as [4]

$$\frac{\boldsymbol{u}^{t+\frac{\Delta t}{2}} - \boldsymbol{u}^{t-\frac{\Delta t}{2}}}{\Delta t} = \frac{q}{m}\left(\boldsymbol{E}^t + \frac{\boldsymbol{u}^{t+\frac{\Delta t}{2}} + \boldsymbol{u}^{t-\frac{\Delta t}{2}}}{2} \times \boldsymbol{B}_\gamma^t\right), \tag{2}$$

where $\boldsymbol{u} = c\boldsymbol{v}/\sqrt{c^2 - |\boldsymbol{v}|^2}$ and $\boldsymbol{B}_\gamma = c\boldsymbol{B}/\sqrt{c^2 + |\boldsymbol{u}^{t-\frac{\Delta t}{2}}|^2} = c\boldsymbol{B}/\sqrt{c^2 + |\boldsymbol{u}^{t+\frac{\Delta t}{2}}|^2}$. According to Boris [3], the acceleration due to electric and magnetic forces are separated numerically as follows:

$$\boldsymbol{u}^- = \boldsymbol{u}^{t-\frac{\Delta t}{2}} + \frac{q}{m}\boldsymbol{E}^t\frac{\Delta t}{2}, \tag{3a}$$

$$\frac{\boldsymbol{u}^+ - \boldsymbol{u}^-}{\Delta t} = \frac{q}{m}\left(\frac{\boldsymbol{u}^+ + \boldsymbol{u}^-}{2} \times \boldsymbol{B}_\gamma^t\right), \tag{3b}$$

$$\boldsymbol{u}^{t+\frac{\Delta t}{2}} = \boldsymbol{u}^+ + \frac{q}{m}\boldsymbol{E}^t\frac{\Delta t}{2}. \tag{3c}$$

Taking the inner dot product of Eq.(3b) with $(\boldsymbol{u}^+ + \boldsymbol{u}^-)$, we obtain $|\boldsymbol{u}^+|^2 - |\boldsymbol{u}^-|^2 = 0$. This means that the kinetic energy of a charged particle does not change during the gyration in the velocity space by a magnetic field since the magnetic field do not work.

Email address: taka.umeda@nagoya-u.jp (Takayuki Umeda)

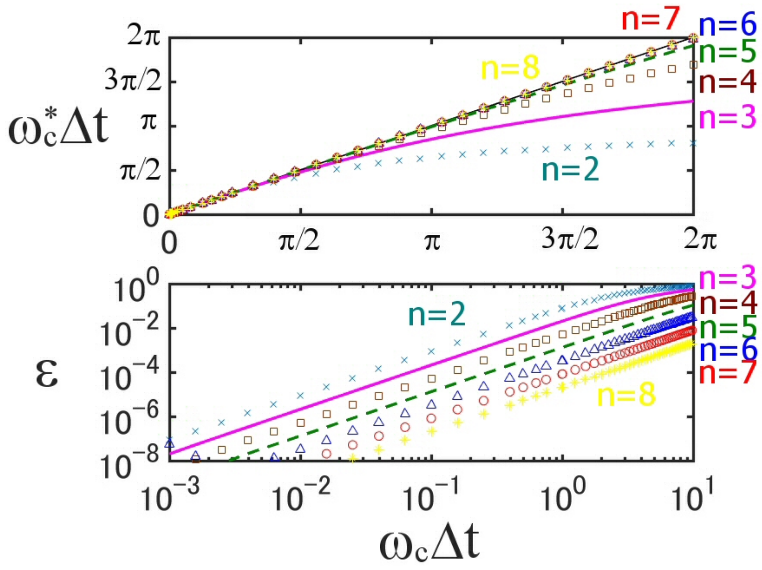

Figure 1: Approximated gyration angle for one time step $\omega_c^*\Delta t$ and the corresponding error $\varepsilon = (\omega_c - \omega_c^*)/\omega_c$ as a function of $\omega_c\Delta t$ for n-step Boris rotation schemes. The x-marks, solid line, square marks, dashed line, triangles, circles, and cross marks correspond to the two-, three-, four-, five-, six-, seven-, and eight-step schemes, respectively.

This paper deals with the Lorentz force equation (3b) only. A matrix inversion is needed for solving Eq.(3b) [5], since this equation takes an implicit form. On the other hand, Boris [3] found a simple approximation of $(\boldsymbol{u}^+ + \boldsymbol{u}^-)/2$ as follows:

$$\beta = \frac{1}{1 + \left(\frac{q}{m}\left|\boldsymbol{B}_\gamma^t\right|\frac{\Delta t}{2}\right)^2}, \tag{4a}$$

$$\frac{\boldsymbol{u}^+ + \boldsymbol{u}^-}{2} \equiv \boldsymbol{u}^\tau \approx \beta\left\{\boldsymbol{u}^- + \frac{q}{m}(\boldsymbol{u}^- \times \boldsymbol{B}_\gamma^t)\frac{\Delta t}{2}\right\}, \tag{4b}$$

where

$$\boldsymbol{u}^+ = \boldsymbol{u}^- + \frac{q}{m}(\boldsymbol{u}^\tau \times \boldsymbol{B}_\gamma^t)\Delta t. \tag{4c}$$

Hereafter, we refer to these procedures as the standard Boris rotation. By using Eq.(4c), we obtain

$$0 = \frac{\boldsymbol{u}^+ - \boldsymbol{u}^-}{\Delta t}\cdot(\boldsymbol{u}^+ + \boldsymbol{u}^-) = \frac{q}{m}\left(\boldsymbol{u}^\tau \times \boldsymbol{B}_\gamma^t\right)\cdot\left\{2\boldsymbol{u}^- + \frac{q}{m}(\boldsymbol{u}^\tau \times \boldsymbol{B}_\gamma^t)\Delta t\right\}. \tag{5}$$

Equation (4a) is the unique solution to the above equation. Note that the procedures (3) and (4) are also called the Buneman-Boris scheme in some references [e.g., 2, 6], since the time-symmetric equation (2) was first discussed by Buneman [4]. It is known that the Bunrman-Boris scheme follows trajectories of charged particles with more accurately than the fourth-order Runge-Kutta scheme [7, 8], although the scheme has the second-order accuracy in time by the leap-frog time-stepping.

The gyration angle for one time step $\omega_c\Delta t$ (where $\omega_c = q|\boldsymbol{B}_\gamma^t|/m$) is approximated by the standard two-step Boris rotation in Eq.(4) as

$$\cos^2\left(\frac{\omega_c^*\Delta t}{2}\right) \approx \beta \quad \text{or} \quad \omega_c^*\Delta t \approx 2\tan^{-1}\left(\frac{q|\boldsymbol{B}_\gamma^t|\Delta t}{2m}\right). \tag{6}$$

The "x" marks in Figure 1 show the approximated gyration angle for one time step $\omega_c^*\Delta t$ by the standard Boris rotation and the corresponding error $\varepsilon = (\omega_c - \omega_c^*)/\omega_c$ as a function of $\omega_c\Delta t$. It is seen that the standard (two-step) Boris rotation has the second-order accuracy in time for a small time step ($\omega_c\Delta t \ll 1$). The error in the gyration angle of the standard

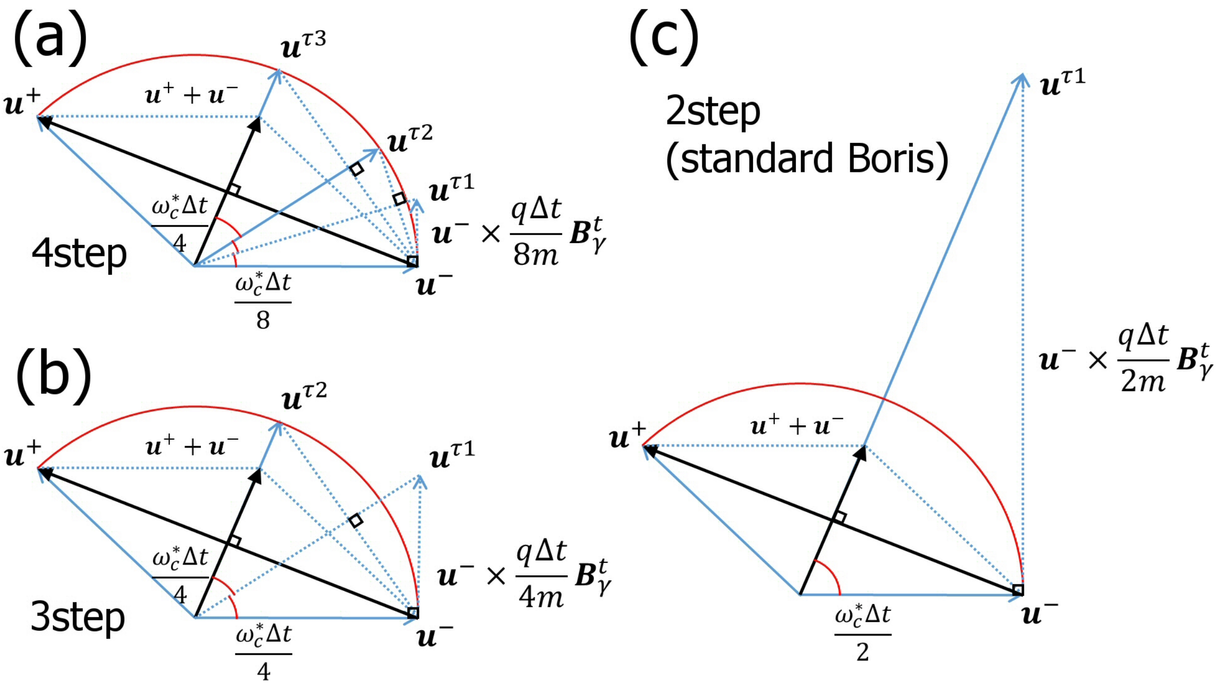

Figure 2: Schematic illustration of the velocity vector change in the four-step (a), the three-step (b), and the standard (two-step) Boris rotation schemes (c).

Boris rotation is 0.66° at the gyration angle of 30°($\omega_c \Delta t \sim 0.5236$). For a larger time step ($\omega_c \Delta t > 1$), on the other hand, the error in the gyration angle is larger and nonlinear.

The present study aims to increase the accuracy of the gyration for large time step of $\omega_c \Delta t > 1$. Recent advances in the implicit particle-in-cell method allows us to use a much larger time step than in the standard explicit one [e.g. 9, 10]. Recent development in supercomputer technologies also allows us to perform full particle-in-cell simulations with a long simulation time of $\omega_{ci} t > 100$. With a realistic mass ratio, the simulation time exceeds $\omega_{ce} t = 180,000$, which corresponds to the time steps of 10^6–10^7. For such a large number of time steps, the numerical error of the entire gyration is not negligible even when the numerical error for one time step is small.

A three-step Boris rotation has been developed in the previous study, which has the same accuracy as the standard (two-step) Boris rotation with a half time step [11]. In the present study, we extend the three-step rotation a general n-step one.

2. Numerical procedures

The numerical procedures of the standard (two-step) Boris rotation are as follows:

$$\boldsymbol{u}^{\tau_1} = \boldsymbol{u}^- + \beta_{(1,2)} \boldsymbol{u}^- \times \frac{q\Delta t}{2m} \boldsymbol{B}_\gamma^t, \tag{7a}$$

$$\boldsymbol{u}^+ = \boldsymbol{u}^- + \beta_{(2,2)} \boldsymbol{u}^{\tau_1} \times \frac{q\Delta t}{m} \boldsymbol{B}_\gamma^t, \tag{7b}$$

where

$$B_2 \equiv \frac{q\Delta t}{2m} \left| \boldsymbol{B}_\gamma^t \right|, \quad \beta_{(1,2)} = 1, \quad \beta_{(2,2)} = \frac{1}{1 + B_2^2}. \tag{7c}$$

The change of the velocity vector by the standard Boris rotation is schematically illustrated in Figure 2c. The velocity vector gyrates from $\boldsymbol{u}^-$ to $\boldsymbol{u}^+$ along a segment of the circle satisfying $|\boldsymbol{u}| = \text{const}$.

The numerical procedures of the three-step Boris rotation [11] are as follows:

$$\boldsymbol{u}^{\tau_1} = \boldsymbol{u}^- + \beta_{(1,3)}\boldsymbol{u}^- \times \frac{q\Delta t}{4m}\boldsymbol{B}^t_\gamma, \tag{8a}$$

$$\boldsymbol{u}^{\tau_2} = \boldsymbol{u}^- + \beta_{(2,3)}\boldsymbol{u}^{\tau_1} \times \frac{q\Delta t}{2m}\boldsymbol{B}^t_\gamma, \tag{8b}$$

$$\boldsymbol{u}^{+} = \boldsymbol{u}^- + \beta_{(3,3)}\boldsymbol{u}^{\tau_2} \times \frac{q\Delta t}{m}\boldsymbol{B}^t_\gamma, \tag{8c}$$

where

$$B_3 \equiv \frac{q\Delta t}{4m}\left|\boldsymbol{B}^t_\gamma\right|, \quad \beta_{(1,3)} = 1, \quad \beta_{(2,3)} = \frac{1}{1+B_3^2}, \quad \beta_{(3,3)} = \beta_{(2,3)}. \tag{8d}$$

The change of the velocity vector by the three-step Boris rotation is schematically illustrated in Figure 2b. The velocity vector gyrates from $\boldsymbol{u}^-$ to $\boldsymbol{u}^+$ via $\boldsymbol{u}^{\tau1}$ along a segment of the circle satisfying $|\boldsymbol{u}|$ = const. In the three-step scheme, $\boldsymbol{u}^{\tau1}$ is obtained by the two-step scheme. The gyration angle is approximated by the three-step Boris rotation as

$$\cos^2\left(\frac{\omega_c^*\Delta t}{4}\right) \approx \beta_{(2,3)} \quad \text{or} \quad \omega_c^*\Delta t \approx 4\tan^{-1}\left(\frac{q|\boldsymbol{B}^t_\gamma|\Delta t}{4m}\right). \tag{9}$$

In the present study, we derived the procedures of the four-step rotation scheme as follows:

$$\boldsymbol{u}^{\tau_1} = \boldsymbol{u}^- + \beta_{(1,4)}\boldsymbol{u}^- \times \frac{q\Delta t}{8m}\boldsymbol{B}^t_\gamma, \tag{10a}$$

$$\boldsymbol{u}^{\tau_2} = \boldsymbol{u}^- + \beta_{(2,4)}\boldsymbol{u}^{\tau_1} \times \frac{q\Delta t}{4m}\boldsymbol{B}^t_\gamma, \tag{10b}$$

$$\boldsymbol{u}^{\tau_3} = \boldsymbol{u}^- + \beta_{(3,4)}\boldsymbol{u}^{\tau_2} \times \frac{q\Delta t}{2m}\boldsymbol{B}^t_\gamma, \tag{10c}$$

$$\boldsymbol{u}^{+} = \boldsymbol{u}^- + \beta_{(4,4)}\boldsymbol{u}^{\tau_3} \times \frac{q\Delta t}{m}\boldsymbol{B}^t_\gamma, \tag{10d}$$

where

$$B_4 = \frac{q\Delta t}{8m}\left|\boldsymbol{B}^t_\gamma\right|, \quad \beta_{(1,4)} = 1, \quad \beta_{(2,4)} = \frac{1}{1+B_4^2}, \quad \beta_{(3,4)} = \beta_{(2,4)},$$
$$\beta_{(4,4)} = \beta_{(3,4)}\left(1 - \beta_{(2,4)}\frac{q^2\Delta t^2}{32m^2}\left|\boldsymbol{B}^t_\gamma\right|^2\right). \tag{10e}$$

We found that $\beta_{(4,4)}$ in Eq.(10e) is the unique solution to Eq.(5). This suggests that the simple solution $\beta_{(l,n)} = \beta_{(l-1,n)}$ is satisfied at the third step only. The change of the velocity vector by the four-step Boris rotation is schematically illustrated in Figure 2a. The velocity vector gyrates from $\boldsymbol{u}^-$ to $\boldsymbol{u}^+$ via $\boldsymbol{u}^{\tau2}$ and $\boldsymbol{u}^{\tau3}$ along a segment of the circle satisfying $|\boldsymbol{u}|$ = const. In the proposed four-step scheme, $\boldsymbol{u}^{\tau2}$ is obtained by the two-step scheme with $\Delta t/4$, and then $\boldsymbol{u}^{\tau3}$ is obtained by the three-step scheme with $\Delta t/2$. The gyration angle is approximated by the proposed four-step Boris rotation as

$$\cos^2\left(\frac{\omega_c^*\Delta t}{8}\right) \approx \beta_{(2,4)} \quad \text{or} \quad \omega_c^*\Delta t \approx 8\tan^{-1}\left(\frac{q|\boldsymbol{B}^t_\gamma|\Delta t}{8m}\right). \tag{11}$$

In Figure 1, the approximated gyration angle for one time step $\omega_c^*\Delta t$ as a function of $\omega_c\Delta t$ and the corresponding error $\varepsilon = (\omega_c - \omega_c^*)/\omega_c$ for the proposed four-step rotation is superimposed. The limit of the gyration angle of the standard two-step Boris rotation for one time step is about 145°, while limit of the gyration angle of the proposed four-step Boris rotation for one time step is about 305°.

We also derived the procedures of the five-step rotation scheme as follows:

$$\boldsymbol{u}^{\tau_1} = \boldsymbol{u}^- + \beta_{(1,5)}\boldsymbol{u}^- \times \frac{q\Delta t}{16m}\boldsymbol{B}^t_\gamma, \tag{12a}$$

$$\boldsymbol{u}^{\tau_2} = \boldsymbol{u}^- + \beta_{(2,5)}\boldsymbol{u}^{\tau_1} \times \frac{q\Delta t}{8m}\boldsymbol{B}^t_\gamma, \tag{12b}$$

$$\boldsymbol{u}^{\tau_3} = \boldsymbol{u}^- + \beta_{(3,5)}\boldsymbol{u}^{\tau_2} \times \frac{q\Delta t}{4m}\boldsymbol{B}^t_\gamma, \tag{12c}$$

$$\boldsymbol{u}^{\tau_4} = \boldsymbol{u}^- + \beta_{(4,5)}\boldsymbol{u}^{\tau_3} \times \frac{q\Delta t}{2m}\boldsymbol{B}^t_\gamma, \tag{12d}$$

$$\boldsymbol{u}^{+} = \boldsymbol{u}^- + \beta_{(5,5)}\boldsymbol{u}^{\tau_4} \times \frac{q\Delta t}{m}\boldsymbol{B}^t_\gamma, \tag{12e}$$

where

$$B_5 = \frac{q\Delta t}{16m}\left|\boldsymbol{B}^t_\gamma\right|, \quad \beta_{(1,5)} = 1, \quad \beta_{(2,5)} = \frac{1}{1+B_5^2}, \quad \beta_{(3,5)} = \beta_{(2,5)},$$

$$\beta_{(4,5)} = \beta_{(3,5)}\left(1 - \beta_{(2,5)}\frac{q^2\Delta t^2}{128m^2}\left|\boldsymbol{B}^t_\gamma\right|^2\right), \quad \beta_{(5,5)} = \beta_{(4,5)}\left(1 - \beta_{(3,5)}\beta_{(2,5)}\frac{q^2\Delta t^2}{32m^2}\left|\boldsymbol{B}^t_\gamma\right|^2\right). \tag{12f}$$

In the five-step rotation, an approximation of $(\boldsymbol{u}^+ + \boldsymbol{u}^-)/2 \approx \beta_{(5,5)}\boldsymbol{u}^{\tau_4}$ is given by the four-step rotation as Eq.(12d). We found that $\beta_{(5,5)}$ in Eq.(12f) is the unique solution to Eq.(5). The gyration angle of the five-step rotation for one time step $\omega_c\Delta t$ is approximated as

$$\cos^2\left(\frac{\omega_c^*\Delta t}{16}\right) \approx \beta_{(2,5)} \quad \text{or} \quad \omega_c^*\Delta t \approx 16\tan^{-1}\left(\frac{q\Delta t}{16m}|\boldsymbol{B}^t_\gamma|\right). \tag{13}$$

By using the same manner, we obtained the procedures of the six-step rotation scheme as follows:

$$\boldsymbol{u}^{\tau_1} = \boldsymbol{u}^- + \beta_{(1,6)}\boldsymbol{u}^{-} \times \frac{q\Delta t}{32m}\boldsymbol{B}^t_\gamma, \tag{14a}$$

$$\boldsymbol{u}^{\tau_2} = \boldsymbol{u}^- + \beta_{(2,6)}\boldsymbol{u}^{\tau_1} \times \frac{q\Delta t}{16m}\boldsymbol{B}^t_\gamma, \tag{14b}$$

$$\boldsymbol{u}^{\tau_3} = \boldsymbol{u}^- + \beta_{(3,6)}\boldsymbol{u}^{\tau_2} \times \frac{q\Delta t}{8m}\boldsymbol{B}^t_\gamma, \tag{14c}$$

$$\boldsymbol{u}^{\tau_4} = \boldsymbol{u}^- + \beta_{(4,6)}\boldsymbol{u}^{\tau_3} \times \frac{q\Delta t}{4m}\boldsymbol{B}^t_\gamma, \tag{14d}$$

$$\boldsymbol{u}^{\tau_5} = \boldsymbol{u}^- + \beta_{(5,6)}\boldsymbol{u}^{\tau_4} \times \frac{q\Delta t}{2m}\boldsymbol{B}^t_\gamma, \tag{14e}$$

$$\boldsymbol{u}^{+} = \boldsymbol{u}^- + \beta_{(6,6)}\boldsymbol{u}^{\tau_5} \times \frac{q\Delta t}{m}\boldsymbol{B}^t_\gamma, \tag{14f}$$

where

$$B_6 = \frac{q\Delta t}{32m}\left|\boldsymbol{B}^t_\gamma\right|, \quad \beta_{(1,6)} = 1, \quad \beta_{(2,6)} = \frac{1}{1+B_6^2}, \quad \beta_{(3,6)} = \beta_{(2,6)},$$

$$\beta_{(4,6)} = \beta_{(3,6)}\left(1 - \beta_{(2,6)}\frac{q^2\Delta t^2}{512m^2}\left|\boldsymbol{B}^t_\gamma\right|^2\right), \quad \beta_{(5,6)} = \beta_{(4,6)}\left(1 - \beta_{(3,6)}\beta_{(2,6)}\frac{q^2\Delta t^2}{128m^2}\left|\boldsymbol{B}^t_\gamma\right|^2\right).$$

$$\beta_{(6,6)} = \beta_{(5,6)}\left\{1 - \beta_{(4,6)}\beta_{(3,6)}\frac{q^2\Delta t^2}{32m^2}\left|\boldsymbol{B}^t_\gamma\right|^2\left(1 - \beta_{(2,6)}\frac{q^2\Delta t^2}{512m^2}\left|\boldsymbol{B}^t_\gamma\right|^2\right)\right\}. \tag{14g}$$

In the six-step rotation, an approximation of $(\boldsymbol{u}^+ + \boldsymbol{u}^-)/2 \approx \beta_{(6,6)}\boldsymbol{u}^{\tau_5}$ is given by the five-step rotation as Eq.(14e). We found that $\beta_{(6,6)}$ in Eq.(14g) is the unique solution to Eq.(5). The gyration angle of the six-step rotation for one time step $\omega_c\Delta t$ is approximated as

$$\cos^2\left(\frac{\omega_c^*\Delta t}{32}\right) \approx \beta_{(2,6)} \quad \text{or} \quad \omega_c^*\Delta t \approx 32\tan^{-1}\left(\frac{q\Delta t}{32m}|\boldsymbol{B}^t_\gamma|\right). \tag{15}$$

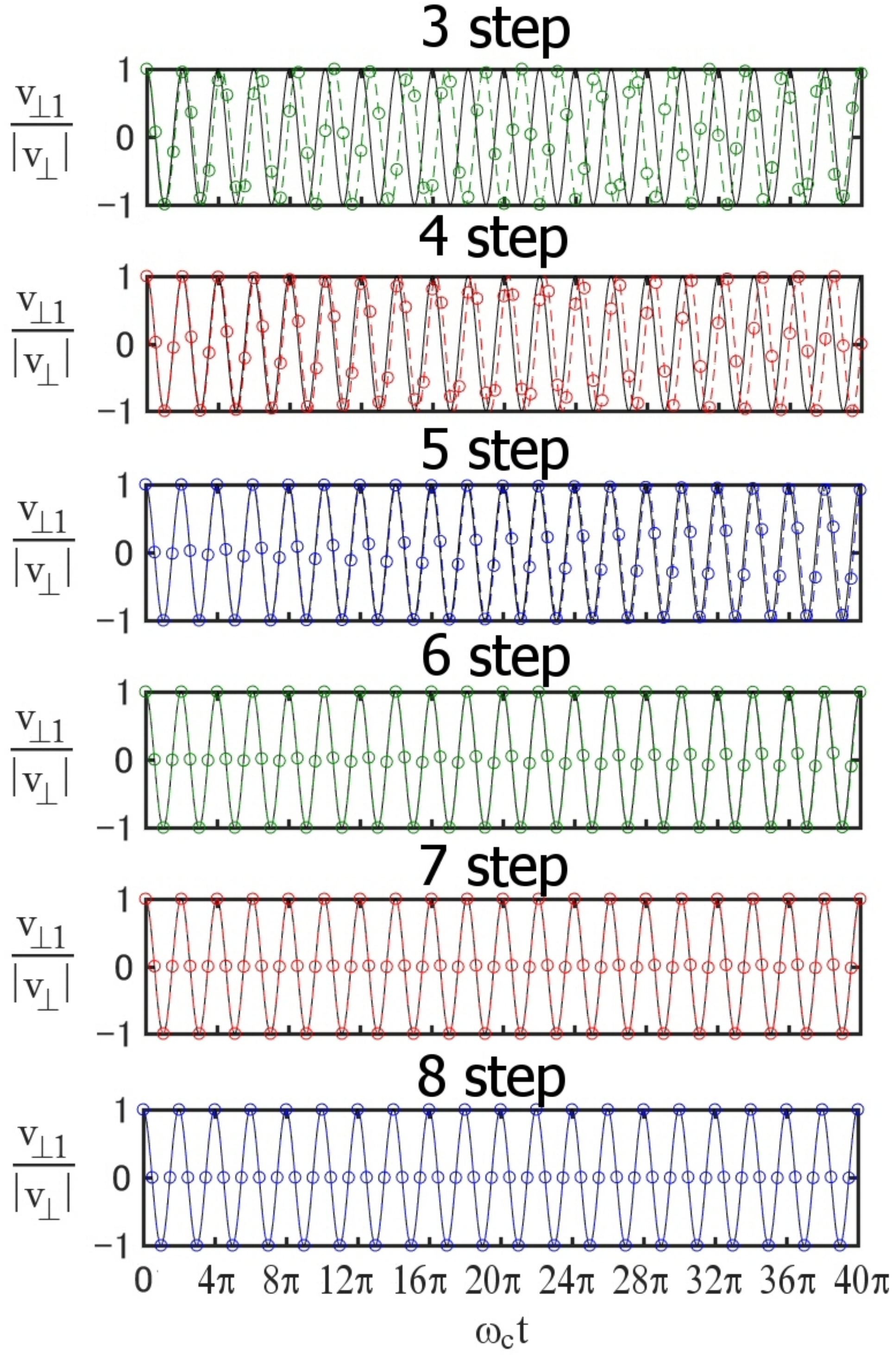

Figure 3: Numerical solutions to the Lorentz force equation with $\omega_c \Delta t = \pi/2$ by using the two-step (standard Boris), the three-step and the four-step rotation schemes. The circles show the results of the numerical test. The dashed lines show the theoretical trajectories given by $\cos \omega_c^* t$. The solid lines show the exact trajectories given by $\cos \omega_c t$.

From these procedures, we derived the recurrence formula for the amplification factor $\beta_{(l,n)}$ at the l-th step of the n-step rotation as follows:

$$\beta_{(l,n)} = \begin{cases} 0 \quad \text{for} \quad l \leq 0, \\ 1 \quad \text{at} \quad l = 1, \\ \dfrac{1}{1+B_n^2} \quad \text{at} \quad l = 2, \\ \beta_{(l-1,n)} \left[1 - 2^{2(l-n)-5}\beta_{(l-2,n)}\beta_{(l-3,n)}B_n^2 \left\{1 - 2^{2(l-n)-9}\beta_{(l-4,n)}\beta_{(l-5,n)}B_n^2 \right.\right. \\ \quad \left.\left. \times\left(1 - 2^{2(l-n)-13}\beta_{(l-6,n)}\beta_{(l-7,n)}B_n^2\left[1 - \cdots\right]\right)\right\}\right] \\ \quad \text{for} \quad n \geq l > 2, \end{cases} \tag{16a}$$

with

$$B_n = \frac{q\Delta t}{2^{n-1}m}\left|\boldsymbol{B}_\gamma^t\right|, \tag{16b}$$

where

$$\boldsymbol{u}^{\tau_l} = \boldsymbol{u}^- + \beta_{(l,n)}\boldsymbol{u}^{\tau_{l-1}} \times \frac{q\Delta t}{2^{n-l}m}\boldsymbol{B}_\gamma^t, \tag{16c}$$

$$\boldsymbol{u}^+ = \boldsymbol{u}^{\tau_n}. \tag{16d}$$

The approximated gyration angle for one time step $\omega_c^*\Delta t$ as a function of $\omega_c\Delta t$ and the corresponding error $\varepsilon = (\omega_c - \omega_c^*)/\omega_c$ for the n-step rotation schemes ($n = 5 - 8$) is superimposed in Figure 1. All of the n-step rotation schemes have the second-order accuracy in time for a small time step ($\omega_c\Delta t \ll 1$) due to the central time difference in Eq.(3b). The accuracy of the gyration angle for a larger time step ($\omega_c\Delta t > 1$) is substantially improved as the number of steps n increases.

3. Numerical Test

A simple numerical test as done in the previous study [11] is conducted to validate the recurrence formula in Eq.(16a) with the seven- and eight-step rotation schemes and to check the consistency between the theoretical approximation of the gyration angle in Figure 1 and the numerical procedures. We use a constant (i.e., time-independent) magnetic field $\boldsymbol{B} = (B_x, B_y, B_z)$ given by uniform random numbers ($0 \leq R \leq 1$). Then, the magnitude of the magnetic field is normalized to unity. We also initiate the velocity vector $\boldsymbol{v} = (v_x, v_y, v_z)$ by a different set of uniform random numbers. We define one of velocity components perpendicular to the magnetic field as,

$$\boldsymbol{v}_{\perp 1}^{t=0} \equiv \boldsymbol{v}^{t=0} - \left(\boldsymbol{v}^{t=0} \cdot \frac{\boldsymbol{B}}{|\boldsymbol{B}|}\right)\frac{\boldsymbol{B}}{|\boldsymbol{B}|}, \tag{17}$$

where $|\boldsymbol{B}| = 1$ in the present numerical test.

Figure 3 shows the time evolution of one of the perpendicular velocity components $v_{\perp 1}^t$ calculated by $v_{\perp 1}^t = \boldsymbol{v}_{\perp 1}^{t=0} \cdot \boldsymbol{v}^t/|\boldsymbol{v}^t|$. We used the three-, four-, five-, six-, seven-, and eight-step rotation schemes with $\omega_c\Delta t = \pi/2$. The circle marks show the numerical results. The dashed lines show the theoretical trajectories given by $\cos\omega_c^* t$. The solid lines show the exact trajectories given by $\cos\omega_c t$.

The result shows that the trajectories of the perpendicular velocity component is on the theoretical trajectories, suggesting the excellent agreement between the numerical calculations and the theory. It is seen that the numerical error is smaller as the number of steps n is larger. The numerical error of the twenty gyrations is not visible with the eight-step rotation. The energy is also well conserved with the n-step schemes within the numerical error of 10^{-14} (not shown).

We also measured the computational time. We solved the Lorentz force equation with 10,000 particles and 10,000 time steps on a single core of an Intel Xeon E5-2697 v4 processor with Intel Fortran ver.17.0. The elapse times with the two-, three-, four-, five-, six-, seven-, and eight- step rotation schemes are 0.1357 sec, 0.2016 sec, and 0.3504 sec, 0.4832 sec, 0.6321 sec, 0.7637 sec, and 0.8661 sec, respectively. Figure 4 shows the computational time of the n-step rotation scheme normalized by the computational time of the standard (two-step) Boris rotation. It is seen that the computational time is almost proportional to the number of steps for $n > 2$.

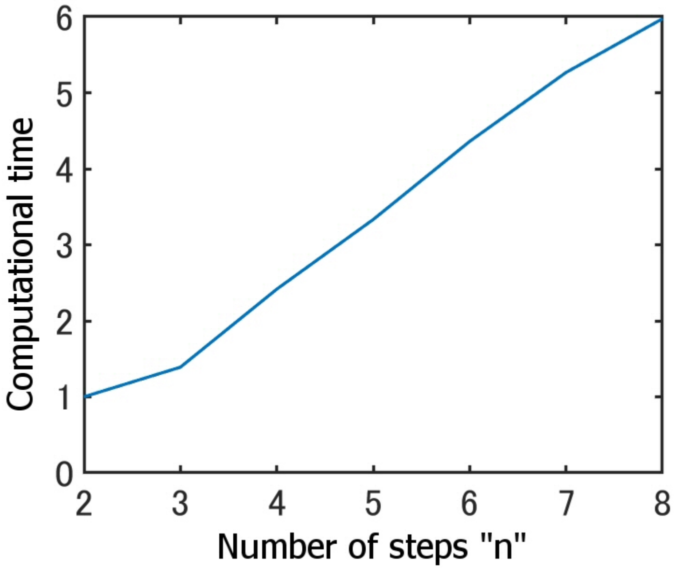

Figure 4: Computational time of the n-step rotation scheme normalized by the computational time of the standard (two-step) Boris rotation.

4. Conclusion

We have developed n-step Boris rotation schemes for solving the Lorentz force equation of charged particle motion. The accuracy of the proposed n-step scheme is 4^{n-2} times higher than that of the standard (two-step) Boris rotation. Although the proposed n-step Boris rotation has the second-order accuracy in time for a small time step ($\omega_c \Delta t \ll 1$), the numerical error in the gyration angle for a large time step ($\omega_c \Delta t > 1$) is much lower than that of the standard Boris rotation. To obtain the same accuracy as the proposed scheme by using the standard Boris rotation, one need 2^{n-1} times $\boldsymbol{v} \times \boldsymbol{B}$ operation with $\Delta t / 2^{n-2}$. On the other hand, the computational time of the n-step rotation is almost proportional to the number of steps for $n > 2$. Hence, the computational cost of the proposed scheme is cheaper as the number of steps n is larger.

In the real space, there exists a plasma with a large magnetization ratio of $\omega_c/\omega_p \gg 1$ near stars, planets and satellites with a strong intrinsic magnetic field. For an example, $\omega_c/\omega_p > 5$ in the terrestrial auroral ionosphere. In such a strongly magnetized plasma, the proposed n-step rotation schemes allow us to use a large $\omega_c \Delta t$. Implementation of the proposed n-step rotation into the entire equation of motion for charged particles, however, is left as a future study. In order to increase the order of accuracy for the time integration, we need to replace the central difference equation (3b) to a higher-order one.

Acknowledgment

This work was supported by MEXT/JSPS under Grant-In-Aid (KAKENHI) for Scientific Research (B) No.JP26287041. This work was conducted as a collaborative research project at the Institute for Space-Earth Environmental Research, Nagoya University.

References

[1] R. W. Hockney, J. W. Eastwood, Computer Simulation Using Particles,McGraw-Hill, New York, 1981.
[2] C. K. Birdsall, A. B. Langdon, Plasma Physics via Computer Simulation, McGraw-Hill, New York, 1985.
[3] J. P. Boris, Relativistic plasma simulation-optimization of a hybrid code, in: Proceedings of 4th Conference on Numerical Simulation of Plasmas, Naval Research Laboratory, Washington D.C., 1970, pp.3–67.
[4] O. Buneman, Time reversible difference procedures, J. Comput. Phys. 1 (1967) 517–535.
[5] T. Tajima, Computational plasma physics: with applications to fusion and astrophysics Addison-Wesley, Boston, 1989.

[6] H. Matsumoto, Y. Omura, Computer Space Plasma Physics, Terra Scientific, Tokyo, 1993.
[7] H. Qin, S. Zhang, J. Liu, Y. Sun, W.M. Tang, Why is Boris algorithm so good?, Phys. Plasmas 20 (2013) 084503.
[8] Y. He, Y. Sun, J. Liu, H. Qin, Volume-preserving algorithms for charged particle dynamics, J. Comput. Phys. 281 (2015) 135–147.
[9] N. Ikeya, Y. Matsumoto, Stability property of numerical Cherenkov radiation and its application to relativistic shock simulations, Publ. Astron. Soc. Japan 67 Y (2015) 64.
[10] G. Lapenta, Exactly energy conserving semi-implicit particle in cell formulation, J. Comput. Phys. 334 (2017) 349–366.
[11] T. Umeda, A three-step Boris integrator for Lorentz force equation of charged particles, Comput. Phys. Comm. 228 (2018) 1–4.